Özge Yüksel Orhan / Hacettepe J. Biol. & Chem., 2021, 49 (1), 57-68

Research Article

Hacettepe Journal of Biology and Chemistry

journal homepage: www.hjbc.hacettepe.edu.tr

Investigation of Biocatalytic Absorption and Ultrasound-Assisted Desorption Performance of CO_2 Capture

CO_2 Yakalamanın Biyokatalitik Absorpsiyon ve Ultrasonik-Destekli Desorpsiyon Performansının İncelenmesi

Özge Yüksel Orhan

Hacettepe University, Department of Chemical Engineering, Ankara, Turkey.

ABSTRACT

The CO_2 absorption-desorption performance of non-aqueous solutions comprising a sterically hindered amine system (2-amino-2-ethyl-1,3-propanediol (AEPD): 1-hexanol) was investigated in a gas-liquid stirred cell reactor under sequential absorption-desorption cycles. The absorption capacity and initial absorption rate were calculated for different concentrations of AEPD: 1-hexanol at 303 K and 2 bar absolute pressure. Increasing the amount of AEPD increased the CO_2 absorption capacity. The biocatalytic effect of a constant amount of carbonic anhydrase (CA) on the CO_2 absorption performance was also investigated, and the CA enzyme was found to increase the total amount of absorbed CO_2. The CO_2 loading of AEPD: 1-hexanol and CA activated AEPD: 1-hexanol were 0.88 and 0.97 mol CO_2/mol AEPD, respectively. CO_2 desorption experiments were performed in different sequences of the same experimental set-up at 363 K and 1.1 bar absolute N_2 pressure. The effect of ultrasonic irradiation on the desorption performance of 0.1 g/L CA catalyzed AEPD: 1-hexanol system was also investigated. It was observed that ultrasonic assistance shortened the desorption time and enhanced the desorption rate. Furthermore, the effectiveness of regeneration, the reusability, and performance loss of AEPD: 1-hexanol, in the presence and absence of CA, were analyzed by Fourier transform infrared spectrometry.

Key Words

CO_2 capture, carbonic anhydrase, FTIR, sterically hindered amine.

ÖZ

Sterik engelli amin sisteminin susuz çözeltisinin (2-amino-2-etil-1,3-propandiol (AEPD): 1-hekzanol) ardışık CO_2 absorpsiyon-desorpsiyon performansı gaz-sıvı karıştırmalı hücre reaktöründe incelenmiştir. Farklı AEPD: 1-hekzanol konsantrasyonları için absorpsiyon kapasitesi ve başlangıç absorpsiyon hızı 303 K ve 2 bar mutlak basınçta hesaplanmıştır. AEPD miktarının artırılması CO_2 absorpsiyon kapasitesini arttırmıştır. Sabit miktarda karbonik anhidrazın (CA) CO2 absorpsiyon performansı üzerindeki biyokatalitik etkisi de araştırılmış, ve CA enziminin toplam absorplanan CO_2 miktarını arttırdığı bulunmuştur. AEPD: 1-hekzanol ve CA ile aktifleştirilen AEPD: 1-hekzanolün CO_2 yüklemesi sırasıyla 0.88 ve 0.97 mol CO_2/mol AEPD bulunmuştur. CO_2 desorpsiyon deneyleri, 363 K ve 1.1 bar mutlak N_2 basıncında aynı deney düzeneğinin farklı dizilimde gerçekleştirilmiştir. Ultrasonik ışınlamanın 0.1 g/L CA katalizli AEPD: 1-hekzanol sisteminin desorpsiyon performansı üzerindeki etkisi de araştırılmıştır. Ultrasonik desteğin desorpsiyon süresini kısalttığı ve desorpsiyon hızını arttırdığı gözlenmiştir. Ayrıca, AEPD:1-Hekzanol sisteminin, CA yokluğunda ve varlığındaki, rejenerasyonun etkinliği, yeniden kullanılabilirliği ve performans kaybı Fourier dönüşümü kızılötesi spektrometresi ile analiz edilmiştir.

Anahtar Kelimeler

CO_2 yakalama, karbonik anhidraz, FTIR, sterik engelli amin.

Article History: Received: Aug 19, 2020; Revised: Oct 12, 2020; Accepted: Oct 12, 2020; Available Online: Nov 20, 2020.

DOI: https://doi.org/10.15671/hjbc.776359

Correspondence to: O. Yuksel Orhan, Department of Chemical Engineering, Hacettepe University, Ankara, Turkey.

E-Mail: oyuksel@hacettepe.edu.tr

INTRODUCTION

The emission of carbon dioxide (CO_2), one of the primary greenhouse gases (GHGs) responsible for global warming, is increasing. CO_2 absorbs less heat per molecule than do other greenhouse gases such as methane (CH_4) or nitrous oxide (N_2O). However, CO_2 is more abundant and stays much longer in the atmosphere [1]. Atmospheric CO_2 concentrations have reached an alarming level of around 410 ppm in 2019, according to the International Energy Agency report [2]. Anthropogenic CO_2 emissions mainly result from the transportation and burning of fossil fuels for energy [3], while electricity generation and the power sector are responsible for the lion's share of non-anthropogenic CO_2 emissions [4]. Therefore, reduction of CO_2 emissions is an important topic on the global agenda to fight climate change.

The absorption–desorption process using aqueous amine solvents has been demonstrated as widely-used methodology for post-combustion CO_2 capture (PCC) [5]. Aqueous 30 wt% monoethanolamine (MEA) is considered a benchmark solution for CO_2 separation from bulk CO_2 gas streams. Even though aqueous amine-based absorbents have good CO_2 absorption characteristics, a large amount of energy is required during regeneration. The regeneration heat for aqueous 30 wt% MEA is around 4 GJ/ton CO_2 [6, 7]. Solvent regeneration is energetically demanding, representing about 70% to 80% of the total energy consumption [8]. The high specific heat of water increases the sensible heat, and the low boiling point of water results in vaporization during the regeneration process, leading to solvent loss [9]. This high energy demand is the driving force behind the development of new solvents with lower regeneration energy consumption. In recent years, there have been several proposals for using water-lean or non-aqueous amine solutions due to their energy-saving potential, but there is still a significant gap from the desired level [7, 10-16]. The widely known organic solvent, 1-hexanol, has a high boiling point but lower heat capacity and vaporization enthalpy than those of water. In the present study, 1-hexanol is proposed as a non-aqueous medium for cyclic CO_2 absorption and desorption.

MEA, a widely known primary amine, shows higher reactivity with CO_2, has low viscosity, and is inexpensive and easily available; however, its corrosive and volatile nature, as well as low CO_2 loading (mol CO_2/mol MEA= 0.5), have necessitated the search for more efficient absorbents [17]. Primary and secondary amines commonly react with CO_2 to form stable carbamate anions, while tertiary amines form bicarbonate ions [18]. Tertiary amines are known to have higher CO_2 loading capacity (mol CO_2/mol amine ≈1.0) but lower thermal stability and low kinetics. In this context, sterically hindered amines (SHAs) have been suggested as a viable alternative to primary, secondary, and tertiary amines as efficient absorbents for carbon capture. SHAs have a functional group located close to the amino group. The resulting steric hindrance produces weaker C-N bonds upon reaction with CO_2, because of which lower energy is required for solvent regeneration [19]. SHAs have been strongly recommended as potential absorbents due to their high theoretical loading capacity of up to 1.0 mol CO_2/mol amine [20]. Although SHAs show lower reaction kinetics than do primary and secondary amines, they show faster reaction kinetics than do tertiary amines [21]. 2-Amino-2-methyl-1-propanol (AMP), which is the sterically hindered form of MEA, has been intensively studied [14, 22-26]. The findings led to the introduction of cost-effective and easily regenerable nonaqueous CO_2 absorbents, based on the sterically hindered primary amine, 2-amino-2-ethyl-1,3-propanediol (AEPD), i.e. AEPD: 1-hexanol solution. AEPD is a potentially useful sterically hindered amine that forms an unstable carbamate upon reaction with CO_2.

Piperazine (PZ) and its derivatives are commonly used promoters to enhance the CO_2 kinetics and absorption capacity [27-30]. This study proposes the use of biocatalysts to promote the CO_2 absorption–desorption process. The ubiquitous occurrence of carbonic anhydrase (CA) enzyme in nature and its kinetic potential make it a good biocatalyst for the reversible reactions between CO_2 and amines. CA from bovine erythrocytes is a widely reported biocatalyst for the CO_2 hydration process. Although there have been many studies on the biocatalytic effect of CA on CO_2 absorption kinetics, the effect of CO_2 loading in gas-liquid reactors has not been examined yet [31-36].

A novel solvent regeneration technique, called the ultrasound-assisted method, was also used to enhance the desorption performance and further reduce the energy consumption. Bubbles produced during the ultrasonic irradiation generated shockwaves, which increased the interfacial area between the gas and the liquid, resulting in enhanced mass transfer [37-40]. This triggered

the degassing action, leading to more efficient removal of CO_2 from the loaded solution. The superior performance of this ultrasound-assisted technique makes it a potentially attractive alternative to the traditional desorption process. The knowledge obtained contributed to the literature, as well as formed the basis for the development of a new generation of more efficient CO_2 capture technologies [39]. This new understanding will help the industry achieve significant savings in terms of both capital and operating costs of CO_2 capture and separation processes, which can significantly reduce the greenhouse gas effects and benefit the environment.

MATERIALS and METHODS

Gas-liquid stirred cell contact reactor

Gas absorption and desorption experiments were performed in a gas-liquid stirred cell reactor (model RD-CSTR 200, Sinerji, Turkey). The experimental set-up consisted of a stainless-steel reactor with a heating jacket, a PID-controlled power control unit, and a data acquisition system (Figure 1). The other important components of the reactor system are a mass flow controller (MFC) and a mass flow meter (MFM). The stainless-steel reactor has a driver motor capable of a stirring rate of 50-500 rpm, along with digital temperature and pressure sensors connected to a data acquisition system. The system can operate under a wide range of temperature and pressure conditions, 293-373 K and 0-10 bar, respectively.

In this study, the CO_2 absorption performance of AEPD: 1-hexanol, in the presence and absence of CA, was investigated with the help of high-precision flowmeters connected to the stirred reactor. The effect of amine concentrations, and the presence of CA enzyme on CO_2 absorption capacity were discussed. During an experimental run, the inlet and outlet flow rates of CO_2 were measured by the MFM and MFC and recorded at 10 s intervals until the MFM values approached the set MFC values. The difference between the inlet and outlet gas streams corresponded to the amount of CO_2 absorbed. The total amount of CO_2 captured by the solvent was calculated by the numerical integration method. This cal-

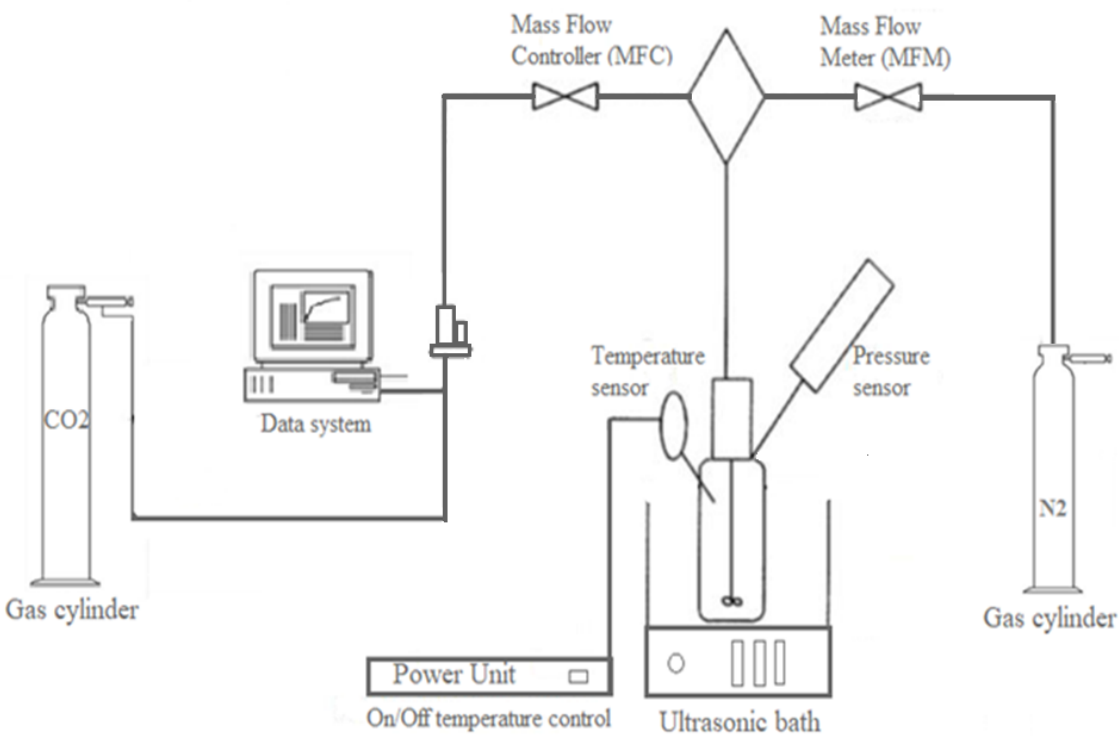

Figure 1. Systematic view of experimental set-up of gas- liquid contact reactor

culated cumulative volumetric amount was converted to absorbed CO_2 in moles by applying the necessary unit changes. The initial absorption rates (mol/s) were calculated from the slopes of the initial and the linear region of the CO_2 loading plot, as shown in Figure 2. Then, this loading rate was divided by the cross-sectional area of the reactor to obtain the general expression for the initial absorption rate (mol/m^2.s). The convenience of the initial absorption rates for a fast reaction was investigated according to the first-order reaction rate equation proposed by Danckwerts [41]. This equation provides solubility, diffusivity and reaction rate in the combined form, A/$(D_A ko)^{0.5}$. To satisfy pseudo first-order conditions, a gas-liquid contact reactor must operate at high concentration ranges of reactants. Opportunely, this concentration range matches to industrial conditions well. It should be noted that, the reaction of CO_2 is actually reversible. However, as in our case, if we take into account only the initial gas absorption (i.e. fresh solvent), the back pressure of dissolved CO_2 will be negligible and Equation 1 will be applicable.

$$\overline{R} = A^* \sqrt{D_A k_o} \quad (1)$$

Where, $\overline{R}$ is the measured CO_2 absorption rate (mol/m^2s), A* is solubility of dissolved CO_2 at the gas-liquid interface (mol/m^3), D_A is the molecular diffusivity of dissolved CO_2 (m^2/s) and k_o is the pseudo-first order reaction rate constant (s^{-1}).

In the absorption experiments, the stirred reactor tank pressure was maintained at 2 bar absolute CO_2 pressure, the temperature was maintained at 303 K, and the MFC was set to 10 sccm. Since the absorption process occurs at constant pressure, there was a continuous CO_2 input into the system, equivalent to the amount of CO_2 absorbed by the reactive solution. The change in the flow rates measured by the MFM and MFC during a typical experimental run, and the CO_2 loading as a function of time are plotted as shown in Figure 2.

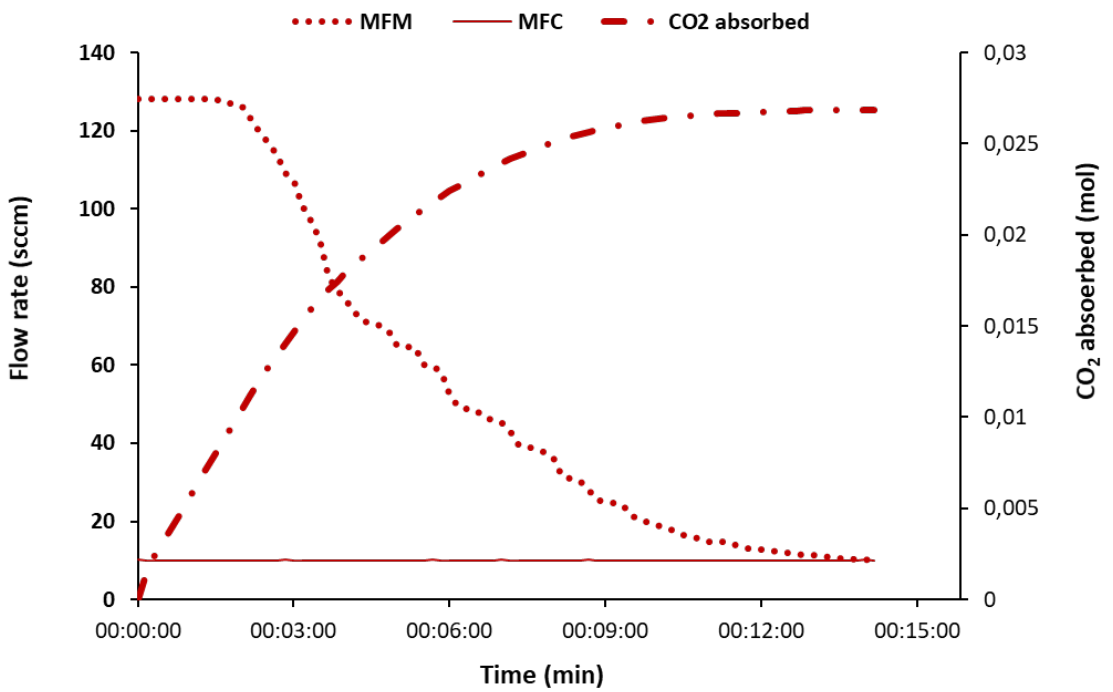

Figure 2. Typical absorption graph of 1.0 M AEPD: 1-hexanol at 303 K and 2 bar.

It was noticed that the absorption rate of the fresh AEPD:1-hexanol solution decreases over time as the solution is saturated with CO_2. The area between the MFC and MFM curves gives the amount of CO_2 absorbed throughout an experimental run. Toward the end of the experiment, the flow value observed in the MFM approached the value of the previously determined MFC and reached equilibrium. Equalization of the MFM and MFC values meant that the solution would not be able to capture any more CO_2.

In addition, different sequences of the same experimental set-up were used to test the reusability of the solutions and to examine the desorption performance. In the desorption experiments, CO_2 was removed from the loaded solution by simple heating and sweeping with an inert gas such as nitrogen (N_2). CO_2 desorption experiments on AEPD:1-hexanol systems, for different concentrations, were performed at 363 K and 1.1 bar absolute N_2 pressure. Ultrasound-assisted desorption experiments were performed in a Bandelin, DL 514 BH model ultrasonic bath with a constant wave frequency of 37 kHz, at 333 K and 1.1 bar absolute N_2 pressure.

In order to investigate the reversibility and performance losses of the SHA solutions, the consecutive absorption-desorption experiments were repeated for 3 cycles. In addition, Fourier infrared transform (FTIR) spectroscopy analyses were performed to demonstrate the regeneration effectiveness and the cyclic performance of CO_2-rich and CO_2-lean SHA solutions in the presence and absence of CA. An FTIR analyzer (Thermo Scientific- NICOLET 6700) was used for detecting the functional groups and characterizing the chemical bonds. Further details of the gas-liquid contact reactor and experimental procedure can be found in the literature [12, 42, 43].

RESULTS and DISCUSSION

Absorption-desorption performance

Gas absorption experiments on the 30 mL AEPD: 1-hexanol system in the presence and absence of CA were performed at 303 K and 2 bar CO_2 absolute pressure in a gas-liquid contact reactor. The AEPD: 1-hexanol system was exposed to at least 3 capture and release cycles in order to investigate its reusability and cyclic capacity. Each experimental set was repeated 3 times and the average of 3 replicate experiments were represented. The absorption capacity and initial absorption rate of the consecutive absorption-desorption experiments for the 0.5 M AEPD: 1-hexanol system are summarized in Table 1. The highest CO_2 loading capacity was reached in the first absorption cycle whereupon a slight decrease was observed in subsequent cycles (Table 1). The absorption capacity loss of the AEPD: 1-hexanol system after the third regeneration cycle was found to be 25%. This can be referred to the incomplete removal of CO_2 during desorption cycle, which was carried out at 363 K and 1.1 bar absolute pressure.

Table 1. Cyclic absorption capacities and initial absorption rate of 0.5 M AEPD: 1-hexanol.

0.5 M AEPD: 1-hexanol: CA	Absorption capacity (mol)	Initial absorption rate (kmol/m^2.s) x (10^5)
1st Absorption	0.0126	1.84
2nd Absorption	0.0104	1.29
3rd Absorption	0.0091	1.14

Table 2. Cyclic absorption capacities and initial absorption rate of 0.75 M AEPD: 1-hexanol.

0.75 M AEPD: 1-hexanol	Absorption capacity (mol)	Initial absorption rate (kmol/m^2.s) x (10^5)
1st Absorption	0.0197	1.59
2nd Absorption	0.0178	1.47
3rd Absorption	0.0149	1.31

Table 3. Cyclic absorption capacities and initial absorption rate of 1.0 M AEPD: 1-hexanol.

1.0 M AEPD: 1-hexanol	Absorption capacity (mol)	Initial absorption rate (kmol/m^2.s) x (10^5)
1st Absorption	0.0267	2.27
2nd Absorption	0.0241	1.98
3rd Absorption	0.0206	1.63

Furthermore, a reduction in the initial absorption rate was observed with a decrease in the absorption capacity. The absorption capacity and initial absorption rate of 0.75 M AEPD: 1-hexanol and 1.0 M AEPD: 1-hexanol systems are reported in Tables 2 and 3, respectively.

As expected, the absorption capacity increased with increasing concentrations of the SHA, as shown in Tables 2 and 3. However, no such analogy was observed for the initial absorption rates.

CO_2 absorption experiments of the CA-activated AEPD: 1-hexanol system were performed at 303 K and 2 bar absolute pressure. The absorption capacity and initial absorption rate for different concentrations of the CA-catalyzed AEPD: 1-hexanol system are presented in Tables 4-6. The amount of CA enzyme added to various concentrations of the AEPD: 1-hexanol system was set at 0.1 g/L. Desorption experiments were performed at 333 K to avoid the denaturation of the CA enzyme. As is evident from Tables 4-6, the highest CO_2 loading capacity was observed in the first absorption, after which a slight decrease was observed in the subsequent absorption cycles. The absorption capacity loss of the CA-activated AEPD: 1-hexanol systems after the third regeneration cycle was found to be 15%.

Both the CO_2 absorption capacity and the initial absorption rate of the CA-catalyzed AEPD: 1-hexanol system were higher than those of the uncatalyzed system. In order to calculate the actual stoichiometry of the reaction between CO_2 and the AEPD: 1-hexanol systems, the first CO_2 absorption capacity was plotted against the corresponding amount of AEPD (Figure 3).

Table 4. Cyclic absorption capacities and initial absorption rate of 0.5 M AEPD: 1-hexanol system catalysed by 0.1 g/L CA.

0.5 M AEPD: 1-hexanol: CA	Absorption capacity (mol)	Initial absorption rate (kmol/m^2.s) x (10^5)
1st Absorption	0.0144	2.36
2nd Absorption	0.0132	2.21
3rd Absorption	0.0121	1.85

Table 5. Cyclic absorption capacities and initial absorption rate of 0.75 M AEPD: 1-hexanol system catalysed by 0.1 g/L CA.

0.75 M AEPD: 1-hexanol: CA	Absorption capacity (mol)	Initial absorption rate (kmol/m^2.s) x (10^5)
1st Absorption	0.0219	2.41
2nd Absorption	0.0208	2.25
3rd Absorption	0.0189	2.18

Table 6. Cyclic absorption capacities and initial absorption rate of 1.0 M AEPD: 1-hexanol system catalysed by 0.1 g/L CA.

1.0 M AEPD: 1-hexanol: CA	Absorption capacity (mol)	Initial absorption rate (kmol/m^2.s) x (10^5)
1st Absorption	0.0289	2.54
2nd Absorption	0.0263	2.37
3rd Absorption	0.0247	2.21

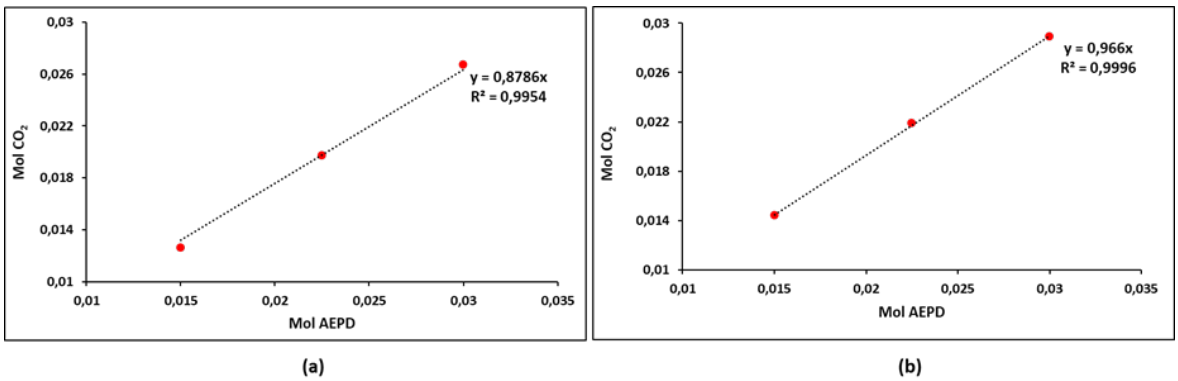

Figure 3. CO_2 loading graphs of (a) AEPD: 1-hexanol system (b) AEPD: 1-hexanol system catalysed by 0.1 g/L CA at 303 K.

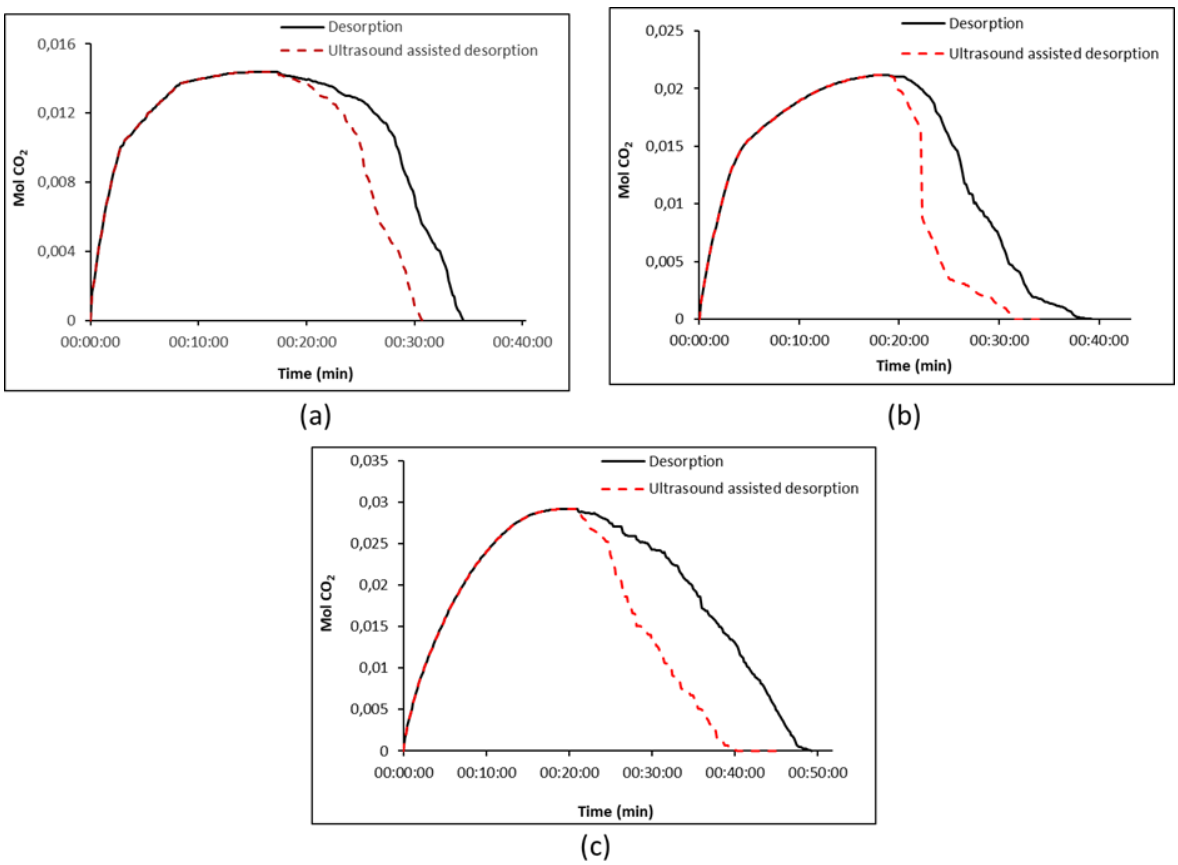

Figure 4. Ultrasound-assisted desorption performances for (a) 0.5 M AEPD: 1-hexanol system catalysed by 0.1 g/L CA (b) 0.75 M AEPD: 1-hexanol system catalysed by 0.1 g/L CA (c) 1.0 M AEPD: 1-hexanol system catalysed by 0.1 g/L CA.

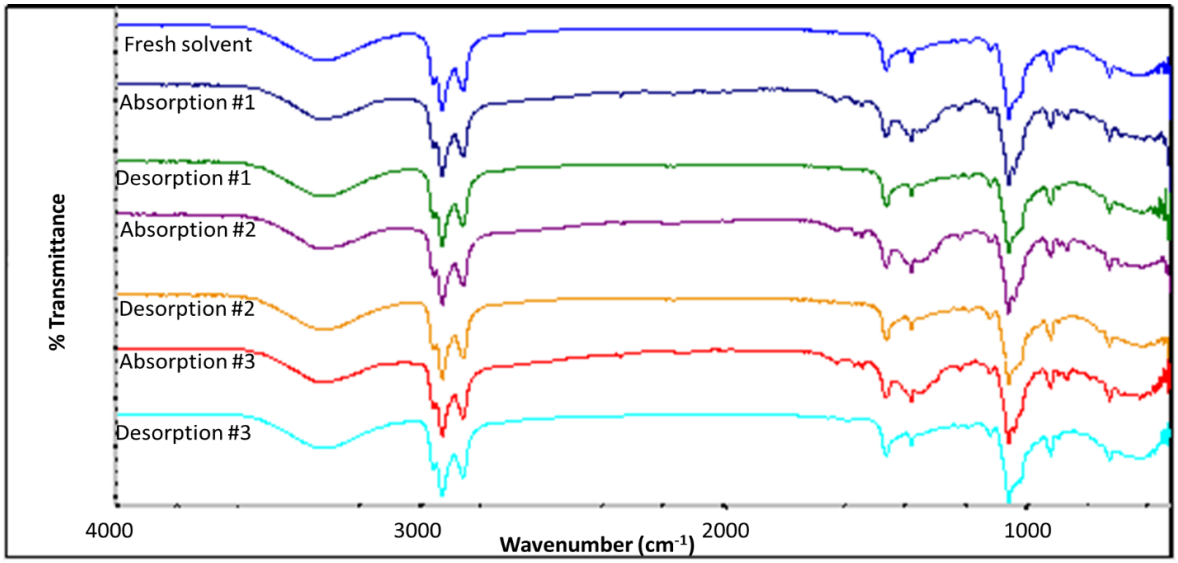

Figure 5. FTIR spectrum of AEPD: 1-hexanol system for 3 absorption-desorption cycles.

AEPD: 1-hexanol is capable of capturing 0.88 moles of CO_2 per mole of AEPD and AEPD: 1-hexanol system catalyzed by 0.1 g/L CA is capable of capturing 0.97 moles of CO_2 per mole of AEPD (Figure 3). The CO_2 absorption capacities for the AEPD: 1-hexanol systems are much higher than the theoretical value of 0.5 mol CO_2/mol MEA. [44]. As per the literature, the CO_2 loading of tertiary amines is close to 0.9 mol CO_2/mol amine, except for MDEA [44]. The CO_2 loading in aqueous MDEA allowed for the capture of 0.63 mol CO_2/mol MDEA, as reported by Jaafari et al., and 0.52 mol CO_2/mol MDEA, as reported by Hadri et al. [6, 29]. The CO_2 absorption capacity of AMP in ethane-1,2-diol was reported to be 0.71 by Im et al. [45]. These results indicate that the loading capacity of a non-aqueous solution of a sterically hindered primary amine (AEPD: 1-hexanol) was superior to that of the benchmark CO_2 capturing agents. This in turn implies that if AEPD: 1-hexanol systems are employed, either in the presence or absence of CA, the solvent circulation rate of an absorber-desorber system will be accordingly decreased.

Ultrasound-assisted desorption studies

Ultrasound-assisted desorption studies were performed in a gas-liquid stirred cell contact reactor under 37 kHz ultrasonic irradiation. CO_2 absorption was carried out at 303 K and 2 bar absolute pressure, desorption at 333 K and 1.1 bar absolute pressure, and ultrasound-assisted desorption at 333 K and 1.1 bar absolute pressure. The experiments on the AEPD: 1-hexanol systems were performed in the presence of 0.1 g/L CA. The experimental results for the absorption and desorption performed under the abovementioned conditions showed that the CO_2 loading and absorption time increase with an increase in the AEPD concentration for each solvent system (Figure 4).

From the above results, it can be concluded that ultrasound-assisted desorption of the 0.1 g/L CA-catalyzed AEPD: 1-hexanol system is beneficial in terms of enhancement of both the CO_2 desorption rate and the CO_2 desorption capacity. It was observed that ultrasound irradiation significantly shortened the CO_2 desorption time for biocatalytic CO_2 capture by AEPD: 1-hexanol. Ultrasonic irradiation in the desorption process intensified bubble formation and decreased the gas-liquid mass transfer resistance, especially at the initial stage.

FTIR analyses

FTIR analyses were performed to study the regenerability and absorption-desorption performance losses of non-SHA solutions. A fresh AEPD:1-hexanol solvent, CO_2-rich solvent after absorption at 303 K and 2 bar pressure, and a CO_2-lean solvent after desorption by heat treatment at 363 K under N_2 bubbling were examined for 3 absorption-desorption cycles. The FTIR spectra of the AEPD: 1-hexanol system are presented in Figure 5.

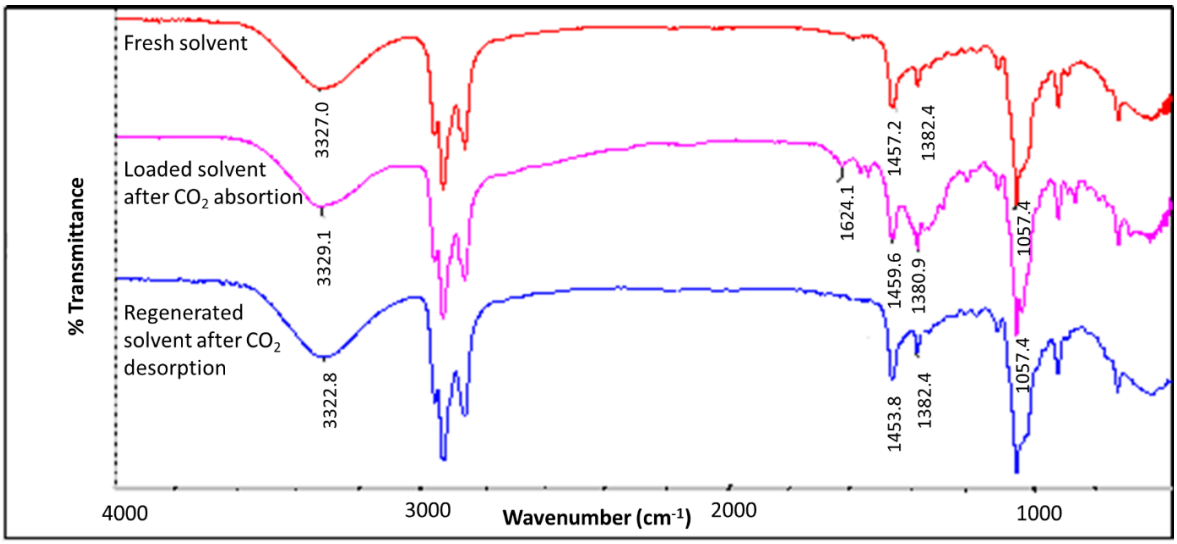

Figure 6. FTIR spectrum of AEPD: 1-hexanol system for the first absorption-desorption cycle.

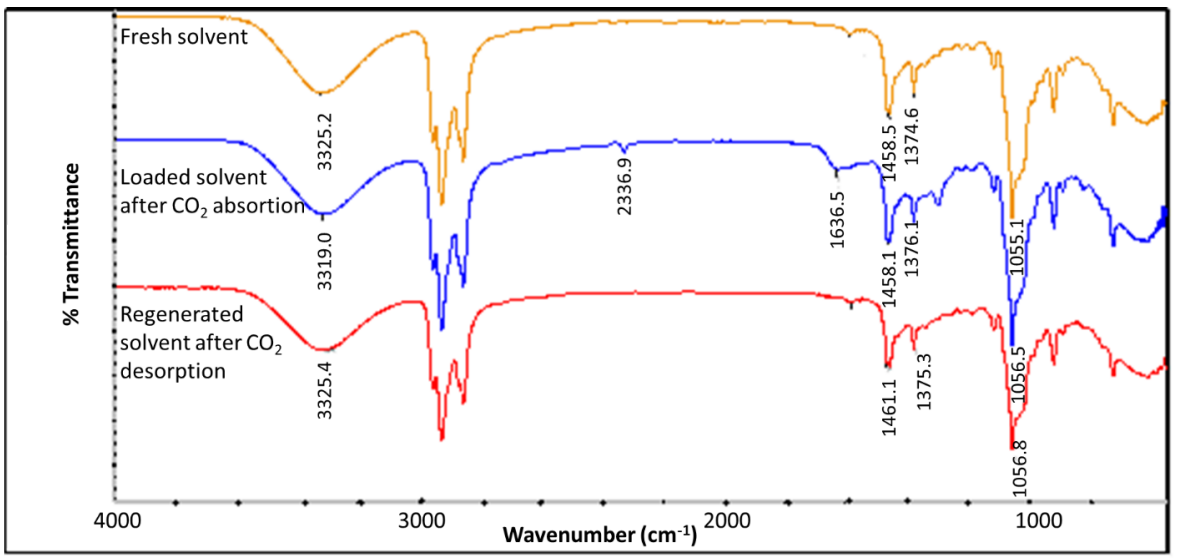

Figure 7. FTIR spectrum of AEPD: 1-hexanol system catalysed by 0.1 g/L CA.

In order to better understand the absorption-desorption performance of the AEPD:1-hexanol system, the FTIR spectrum of the fresh solvent, CO_2-loaded solvent after the first absorption, and CO_2-lean solvent after the first desorption were recorded (Figure 6). Fingerprint peaks for the -OH group were observed in the 3300-3400 cm^{-1} region, while AEPD showed a characteristic peak at ~1050 cm^{-1}. Peaks for the C=O bond in the CO_2-loaded solvent were observed between 1600 and 1650 cm^{-1}. After desorption, the fingerprint peaks for the C=O bond almost disappeared, and the spectrum of the lean solvent became similar to that of the fresh solvent.

The same procedure was repeated to observe the biocatalytic CO_2 absorption-desorption performance of the AEPD: 1-hexanol solution in the presence of 0.1 g/L CA. The FTIR spectra of the fresh solvent, loaded solvent after the first absorption at 303 K and 2 bar, and the lean solvent after the first desorption by heat treatment at 333 K under N_2 bubbling are presented in Figure 7. The characteristic fingerprint peak of the CA enzyme was observed at ~2330 cm^{-1}. The results of the FTIR spectral analyses showed that the CA-activated non-SHA solution can be regenerated at 333 K, which is far below the boiling point of 1-hexanol and other components of the solution, thus providing a significant advantage in preventing solvent loss by evaporation. This behavior could result in significant energy saving for post-combustion CO_2 removal systems, where the traditional solvents require high energy in the form of latent heat.

Finally, ultrasound-assisted desorption was performed at 333 K under N_2 bubbling to study the effect of ultrasound irradiation on the CO_2 desorption performance. The FTIR spectra of the fresh AEPD: 1-hexanol system catalyzed by 0.1 g/L CA, CO_2-loaded solvent after absorption, and CO_2-lean solvent after ultrasound-assisted desorption are shown in Figure 8.

After regeneration of the solution through ultrasound-assisted CO_2 desorption, the loaded spectrum was converted to the lean solvent spectrum, which is almost identical to the spectrum of the fresh solvent.

Conclusion

In the present study, the cyclic absorption and desorption performance of different concentrations of an AEPD:1- hexanol system was studied in a stirred cell gas-liquid reactor. The biocatalytic effect of CA on the absorption capacity was also investigated. With the addition of 0.1 g/L CA, the loading of 0.88 mole CO_2/mol AEPD was enhanced to 0.97 mol CO_2/mol AEPD, which is much higher than the theoretical value of 0.5 mol CO_2/mol MEA for MEA. The obtained results clearly show that the absorption capacity of the AEPD: 1-hexanol system can be enhanced by the addition of small amounts of CA. Thus, CO_2 capture using the proposed solvent system could be achieved with a lesser amount of reactant than that required for traditional amine systems. The AEPD: 1-hexanol system was recy-

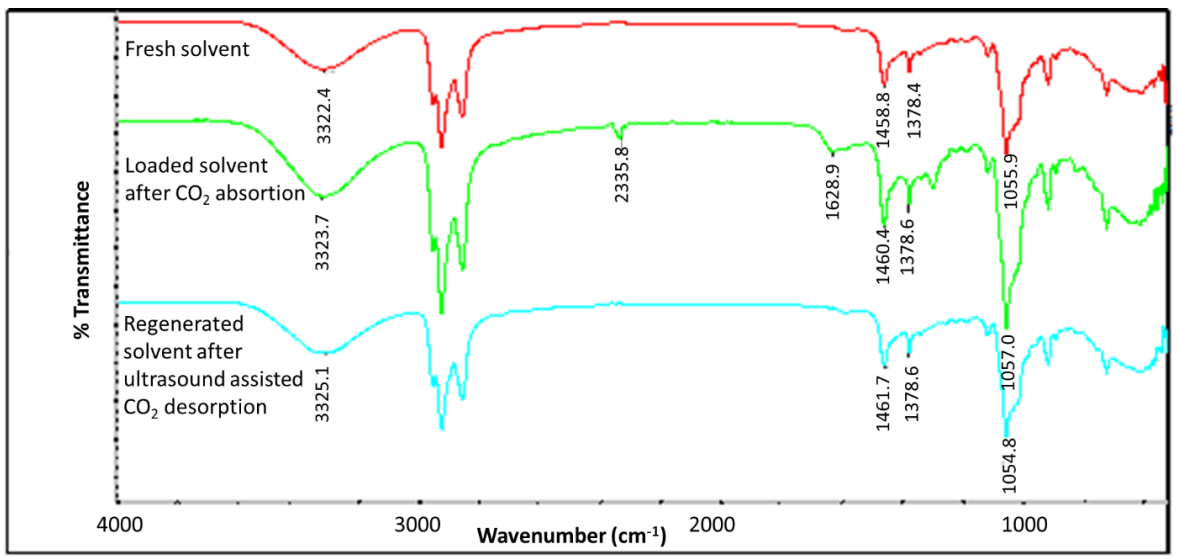

Figure 8. FTIR spectrum of AEPD: 1-hexanol system catalysed by 0.1 g/L CA (in the presence of ultrasound-assisted desorption).

cled at least 3 times by desorption at 363 K and 1.1 bar absolute N_2 pressure. The CA-catalyzed AEPD: 1-hexanol system was also recycled at least 3 times at 333 K, without any considerable loss of capture capacity. These results indicate that this non-aqueous SHA system can be regenerated by simple heating, without boiling or any phase change. Thus, a conventional heavy-duty reboiler may not be required for regeneration. Further, the use of ultrasound-assisted desorption led to a significant increase in the desorption capacity and desorption rate, implying that this technique can minimize the energy consumption for regeneration. Finally, FTIR analyses confirmed the regeneration of the proposed solvent system at much lower temperatures than the boiling points of AEPD or 1-hexanol. To sum up, the AEPD: 1-hexanol solvent system, both in the presence and absence of CA, has potential application as a commercial solvent due to its high CO_2 loading, low volatility, and less energy demand for regeneration by virtue of its non-aqueous nature.

References

1. R. Cassia, M. Nocioni, N. Correa-Aragunde, L. Lamattina, climate change and the impact of greenhouse gasses: CO_2 and NO, friends and foes of plant oxidative stress, Front. Plant Sci., 9 (2018).
2. G.C.e.i. IEA (2020), IEA, Paris https://www.iea.org/articles/global-CO_2-emissions-in-2019.
3. T. Skytt, S.N. Nielsen, B.G. Jonsson, Global warming potential and absolute global temperature change potential from carbon dioxide and methane fluxes as indicators of regional sustainability - A case study of Jamtland, Sweden, Ecol. Indic., 110 (2020).
4. L.M. Romeo, M. Bailera, Design configurations to achieve an effective CO2 use and mitigation through power to gas, J. CO_2 Util., 39 (2020).
5. J. Oexmann, A. Kather, Minimising the regeneration heat duty of post-combustion CO_2 capture by wet chemical absorption: The misguided focus on low heat of absorption solvents, Int. J. Greenh. Gas. Con., 4 (2010) 36-43.
6. N.E.L. Hadri, D.V. Quang, M.R.M. Abu-Zahra, Study of novel solvent for CO_2 post-combustion capture, Enrgy. Proced., 75 (2015) 2268-2286.
7. J.Y. Yang, W. Yu, T. Wang, Z.Z. Liu, M.X. Fang, Process Simulations of the Direct Non-Aqueous Gas Stripping Process for CO_2 Desorption, Ind. Eng. Chem. Res., 59 (2020) 7121-7129.
8. B. Aghel, S. Sahraie, E. Heidaryan, Comparison of aqueous and non-aqueous alkanolamines solutions for carbon dioxide desorption in a microreactor, Energy, 201 (2020).
9. X.Y. Zhu, H.F. Lu, K.J. Wu, Y.M. Zhu, Y.Y. Liu, C.J. Liu, B. Liang, DBU-Glycerol Solution: A CO_2 Absorbent with high desorption ratio and low regeneration energy, Environ. Sci. Technol., 54 (2020) 7570-7578.
10. M.C. Ozturk, O.Y. Orhan, E. Alper, Kinetics of carbon dioxide binding by 1,1,3,3-tetramethylguanidine in 1-hexanol, Int. J. Greenh. Gas Con., 26 (2014) 76-82.
11. O.Y. Orhan, H. Tankal, H. Kayi, E. Alper, Kinetics of CO_2 capture by carbon dioxide binding organic liquids: Experimental and molecular modelling studies, Int. J. Greenh. Gas. Con., 49 (2016) 379-386.
12. M. Ozkutlu, O.Y. Orhan, H.Y. Ersan, E. Alper, Kinetics of CO_2 capture by ionic liquid-CO_2 binding organic liquid dual systems, Chem. Eng. Process., 101 (2016) 50-55.
13. O.Y. Orhan, C.S. Ume, E. Alper, The absorption kinetics of CO_2 into ionic liquid-CO_2 binding organic liquid and hybrid solvents, Green. Energy. Technol., (2017) 241-261.
14. B.H. Lv, K.X. Yang, X.B. Zhou, Z.M. Zhou, G.H. Jing, 2-Amino-2-methyl-1-propanol based non-aqueous absorbent for energy-efficient and non-corrosive carbon dioxide capture, Appl. Energ., 264 (2020).
15. F. Bougie, D. Pokras, X.F. Fan, Novel non-aqueous MEA solutions for CO_2 capture, Int. J. Greenh. Gas Con., 86 (2019) 34-42.
16. C.X. Li, X.Q. Shi, S.F. Shen, Performance evaluation of newly developed absorbents for solvent-based carbon dioxide Capture. Energy & Fuels, 33 (2019) 9032-9039.
17. P.V. Kortunov, M. Siskin, M. Paccagnini, H. Thomann, CO2 Reaction mechanisms with hindered alkanolamines: control and promotion of reaction pathways, Energ. Fuel., 30 (2016) 1223-1236.
18. W. Conway, S. Bruggink, Y. Beyad, W.L. Luo, I. Melian-Cabrera, G. Puxty, P. Feron, CO_2 absorption into aqueous amine blended solutions containing monoethanolamine (MEA), N,N-dimethylethanolamine (DMEA), N,N-diethylethanolamine (DEEA) and 2-amino-2-methyl-1-propanol (AMP) for post-combustion capture processes, Chem. Eng. Sci. 126 (2015) 446-454.
19. S. Camino, F. Vega, L.M.G. Fernandez, M. Cano, J.A. Camino, B. Navarrete, Kinetic evaluation of sterically hindered amines under partial oxy-combustion conditions, J. Chem. Technol. Biotechnol., (2020).
20. F. Bougie, M.C. Iliuta, Sterically Hindered Amine-Based Absorbents for the Removal of CO_2 from Gas Streams. J. Chem. Eng. Data, 57 (2012) 635-669.
21. S.J. Yoon, H. Lee, J.H. Yoon, J.G. Shim, J.K. Lee, B.Y. Min, H.M. Eum, Kinetics of absorption of carbon dioxide into aqueous 2-amino-2-ethyl-1,3-propanediol solutions, Ind. Eng. Chem. Res., 41 (2002) 3651-3656.
22. M.P. Patil, P.D. Vaidya, Aqueous mixtures of AMP, HMDA-N,N'-dimethyl and TEG for CO_2 separation: a study on equilibrium and reaction kinetics, Chem. Eng. Commun., (2019).
23. N. Prasongthum, P. Natewong, P. Reubroycharoen, R. Idem, Solvent regeneration of a CO_2-loaded BEA-AMP Bi-blend amine solvent with the aid of a solid bronsted Ce(SO4)(2)/ZrO_2 superacid catalyst, Energ. Fuel., 33 (2019) 1334-1343.
24. M.P. Patil, P.D. Vaidya, Kinetics of CO_2 Absorption into Aqueous AMP/HMDA/TEG Mixtures, Chemistryselect, 3 (2018) 195-200.
25. S.K. Dash, A.N. Samanta, S.S. Bandyopadhyay, Simulation and parametric study of post combustion CO_2 capture process using (AMP plus PZ) blended solvent, Int. J. Greenh. Gas Con., 21 (2014) 130-139.
26. A.K. Saha, S.S. Bandyopadhyay, A.K. Biswas, Kinetics of absorption of CO_2 into aqueous-solutions of 2-amino-2-methyl-1-oropanol, Chem. Eng. Scie., 50 (1995) 3587-3598.

27. S. Kumar, M.K. Mondal, Selection of efficient absorbent for CO_2 capture from gases containing low CO_2, Korean J. Chem. Eng., 37 (2020) 231-239.
28. S. Ullah, H. Suleman, M.S. Tahir, M. Sagir, S. Muhammad, A.G. Al-Sehemi, M.U.R. Zafar, F.A.A. Kareem, A.S. Maulud, M.A. Bustam, Reactive kinetics of carbon dioxide loaded aqueous blend of 2-amino-2-ethyl-1,3-propanediol and piperazine using a pressure drop method, Int. J. Chem. Kinet., 51 (2019) 291-298.
29. L. Jaafari, B. Jaffary, R. Idem, Screening study for selecting new activators for activating MDEA for natural gas sweetening, Sep. Purif. Technol., 199 (2018) 320-330.
30. O.Y. Orhan, E. Alper, Kinetics of carbon dioxide binding by promoted organic liquids, Chem. Eng. Technol., 38 (2015) 1485-1489.
31. T. Sharma, S. Sharma, H. Kamyab, A. Kumar, Energizing the CO_2 utilization by chemo-enzymatic approaches and potentiality of carbonic anhydrases: A review, J. Clean. Prod., 247 (2020).
32. N. Cihan, O.Y. Orhan, The enhanced enzymatic performance of carbonic anhydrase on the reaction rate between CO_2 and aqueous solutions of sterically hindered amines, Greenh. Gases, (2020).
33. B. Liu, X. Luo, Z.W. Liang, W. Olson, H.L. Liu, R. Idem, P. Tontiwachwuthikul, The development of kinetics model for CO_2 absorption into tertiary amines containing carbonic anhydrase, Aiche J., 63 (2017) 4933-4943.
34. Y.Z. Wang, M.F. Li, Z.P. Zhao, W.F. Liu, Effect of carbonic anhydrase on enzymatic conversion of CO_2 to formic acid and optimization of reaction conditions, J. Mol. Catal. B-Enzym., 116 (2015) 89-94.
35. I. Iliuta, M.C. Iliuta, F. Larachi, Catalytic CO_2 hydration by immobilized and free human carbonic anhydrase II in a laminar flow microreactor - Model and simulations, Sep. Purif. Technol., 107 (2013) 61-69.
36. P. Mirjafari, K. Asghari, N. Mahinpey, Investigating the application of enzyme carbonic anhydrase for CO_2 sequestration purposes, Ind. Eng. Chem. Res., 46 (2007) 921-926.
37. J.R. Ying, D.A. Eimer, A. Mathisen, F. Brakstad, H.A. Haugen, Ultrasound intensify CO_2 desorption from pressurized loaded monoethanolamine solutions. II. Optimization and cost estimation, Energy, 173 (2019) 218-228.
38. X.K. Xing, C.B. Feng, Enhancing CO_2 desorption from crude oil by ultrasound, Ultrasonics, 84 (2018) 74-80.
39. O. Yuksel Orhan, Keles, Y., Yavuz Ersan, H., Alper, E., Ultrasound-assisted desorption of CO_2 from carbon dioxide binding organic liquids, Energy Procedia 114 (2017) 66-71.
40. K. Tanaka, H. Okawa, T. Fujiwara, T. Kato, K. Sugawara, Desorption of CO_2 from low concentration monoethanolamine solutions using calcium chloride and ultrasound irradiation, Jpn. J. Appl. Phys., 54 (2015).
41. P.V. Danckwerts, Reaction of CO_2 with Ethanolamines, Chem. Eng. Sci., 34 (1979) 443-446.
42. O.Y. Orhan, E. Alper, Kinetics of reaction between CO_2 and ionic liquid-carbon dioxide binding organic liquid hybrid systems: Analysis of gas-liquid absorption and stopped flow experiments, Chem. Eng. Sci., 170 (2017) 36-47.
43. O.Y. Orhan, M.C. Ozturk, A. Seker, E. Alper, Kinetics and performance studies of a switchable solvent TMG (1,1,3,3-tetramethylguanidine)/1-propanol/carbon dioxide system, Turk. J. Chem., 39 (2015) 13-24.
44. H.X. Gao, Z.Y. Wu, H. Liu, X. Luo, Z.W. Liang, Experimental studies on the effect of tertiary amine promoters in aqueous monoethanolamine (MEA) solutions on the absorption/stripping performances in post-combustion CO_2 capture, Energ. Fuel., 31 (2017) 13883-13891.
45. J. Im, S.Y. Hong, Y. Cheon, J. Lee, J.S. Lee, H.S. Kim, M. Cheong, H. Park, Steric hindrance-induced zwitterionic carbonates from alkanolamines and CO_2: highly efficient CO_2 absorbents, Energy Environ. Sci., 4 (2011) 4284-4289.